Efficient Wideband Sonar Parameter Estimation Using a Single Slice of Radon-Ambiguity Transform

Md. Raihan Sharif and Saman S. Abeysekera, *Member*, *IEEE*

School of Electrical and Electronic Engineering
Nanyang Technological University, Nanyang Avenue, Singapore 639798
E-mail: smraihan@pmail.ntu.edu.sg, esabeysekera@ntu.edu.sg

ABSTRACT

A novel efficient technique based on Radon-ambiguity transform (RAT) for time delay and Doppler stretch estimation is presented in this paper. The proposed approach combines the narrowband ambiguity function (NAF), the wideband ambiguity function (WAF), and the Radon transform (RT) to estimate multiple targets in noisy environments. The main ridges of NAF represent straight lines whose slopes depend on the Doppler rates of the moving targets. These lines could be effectively detected by computing the RT of the NAF for all possible angles. However, the computation of RT for all possible angles is computationally exhaustive. It is shown in this paper that without calculating the entire RAT, it is possible to estimate target parameters using only a single slice of RAT i.e. using an appropriate projection of the NAF. The resolution issue and the effect of the integration length of RAT in complex white Gaussian noise are also discussed. It is demonstrated that the proposed method can successfully separate overlapping targets.

1. INTRODUCTION

The detection of target return signals is an important problem in many sonar and radar applications. In these applications the signals are usually broadband, and thus the target parameters (time delay and Doppler stretch) are usually estimated via wideband matched filter processing. In this paper, Gaussian-enveloped linear frequency modulated (GLFM) signals are used as the transmitted signal as they are known to possess very good resolution properties for target parameter estimation [4]–[5].

Detection of monocomponent linear frequency modulated (LFM) signal in noise-free environment is a relatively simple task. However, detection of multicomponent LFM signals in the presence of noise requires techniques that are immutable to noise interferences. The Wigner distribution (WD) has been found to be useful for analyzing and detecting nonstationary signals [8]. But in multicomponent signals condition, the WD suffers from cross-terms interference seriously [2]. The RT [1]–[3] of a time-frequency distribution produces local areas of signal concentration that facilitate interpretation of multicomponent signals. The major advantages of RT are that lines are allowed to intersect and it is very robust to noise. In [1], the Radon-Wigner transform (RWT) which is equivalent to the dechirp method has been used to analyze time-varying nonstationary signals. But RWT is the task of tracking straight lines in the time-frequency plane into locating maxima in a *2-d* plane, which is a computationally intensive technique. In [2]–[3], it was assumed that all directions of interest pass through the origin of the ambiguity plane and only the received signal was used in the processing. Under this special assumption delay and Doppler cannot be estimated simultaneously. Moreover, time delay cannot be measured by using only the received signal. But in many cases we may need to estimate both time delay and Doppler stretch, simultaneously.

In this paper, we propose RAT technique that combines the NAF and RT to estimate multiple GLFM sonar target parameters simultaneously. We also show that RAT in conjunction with a *1-d* search on the WAF achieves the Cramer-Rao lower bound (CRLB) for parameter estimation.

2. WIDE AND NARROWBAND AMBIGUITY FUNCTIONS OF GLFM SIGNALS

Consider a transmitter that transmits a signal $s(t)$. Then the received signal from a single scatterer is given by

$$r(t) \approx s[\alpha(t-\tau)] \tag{1}$$

where α is the time scaling and τ is the time delay. The form of the signal in (1) is called the wideband model. The wideband model can also be approximated by the narrowband model [6] as

$$r(t) \approx s(t-\tau)\exp(j2\pi f t)\,. \tag{2}$$

With this model, time scaling the signal by α is approximated by a Doppler shift, f. For a signal with carrier frequency, k, the approximation is [6]

$$f \approx (\alpha-1)k \tag{3}$$

For wideband signals the target detection is usually performed using the signal $r(t)$ via a matched filter processing approach in the delay-scale (τ,α) domain. The delay-scale domain matched filtering is described by the following

$$\rho_{rs}(\tau,\alpha) = \sqrt{\alpha}\int_{-\infty}^{+\infty} r(t)s^*[\alpha(t-\tau)]dt\,. \tag{4}$$

Equation (4) defines the WAF between the transmitted and the received signals. Note that the NAF between the transmitted and the received signals is expressed in a different form, i.e.

$$\xi_{rs}(\tau,f) = \int_{-\infty}^{+\infty} r(t)s^*(t-\tau)\exp(-j2\pi f t)\,dt\,. \tag{5}$$

The complex form of the transmitted GLFM signal is given by

$$s(t) = \exp\{-\gamma t^2 + j[2\pi kt + \pi\beta t^2]\} \tag{6}$$

where the instantaneous frequency at $t=0$ is given by k; β is the frequency sweep rate; γ is an amplitude scaling.

The detail analytical expressions, a comparative discussion of the delay-Doppler resolution issue, the main ridge characteristics and the behavior of NAF and WAF of GLFM waveforms have been discussed in [4]–[5]. In [4]–[5], it has been shown that

WAF exhibits better resolution properties than NAF in delay-Doppler domain. In the following sections we will use RT in conjunction with NAF and WAF to estimate target parameters.

3. RADON-AMBIGUITY TRANSFORM

The RT of square modulus of NAF is defined as the integral along a straight line defined by a distance ρ (radius) from the origin and angle of inclination θ formed by the ρ and τ axis

$$\Re(\rho,\theta) = \int_{-\infty}^{+\infty} \left|\xi_{rs}(\rho\cos\theta - u\sin\theta, \rho\sin\theta + u\cos\theta)\right|^2 du$$

$$\text{where} \quad -\infty < \rho < \infty \quad \text{and} \quad 0 \le \theta \le \pi . \tag{7}$$

Equation (7) defines the RAT and it represents the sum of $|\xi_{rs}(.)|^2$ along the line located at a distance ρ from the origin. For a given angle θ, the peak position of ρ can be deduced as

$$\rho_p = \tau\cos\theta + f\sin\theta . \tag{8}$$

Equation (8) suggests that for known (ρ_p, θ), $\rho_p = \tau\cos\theta + f\sin\theta$ describes a line passing through the target parameters (τ, f) in the NAF plane. Using the mapping in (3), the corresponding line in the WAF plane is given by

$$\rho_p = \tau\cos\theta + (\alpha - 1)k\sin\theta . \tag{9}$$

Since the echo of a target is a GLFM signal, when more than one targets exist, we can effectively distinguish the targets from each other according to the slope of each line of ambiguity function respectively, as shown in Fig. 1. The targets in Fig. 1 can be detected using the entire RAT, which is shown in Fig. 2 (left window). Note that each target shows a peak in RAT plane at θ_i and ρ_{pi}, where $i = 1, 2, 3$.

The RT of Fig. 1 is calculated for all possible θ. Note that the calculation of RAT for all possible angles is computationally intensive. In the next section we will demonstrate the efficient way of computing the target parameters.

4. PARAMETER ESTIMATION PROCEDURE

Based on (9), without computing the entire RAT, it is possible to estimate parameters using only a single slice of the RAT i.e. using an appropriate projection of the NAF. The appropriate angle for projection, θ_a, can be estimated using *2-d* FFT of the NAF using least square estimation (LSE). Then the RT slice of Fig. 1 is calculated at angle θ_a. The approximate computation of the slope of the main ridge of NAF, m (also slope angle θ_a) using *2-d* FFT can be computed directly from signal without prior computing NAF. After some algebraic manipulation the *2-d* FFT of the squared modulus of NAF in (5) can be deduced as

$$\left|F(u, v)\right| = \left|\int_{-\infty}^{+\infty}\int_{-\infty}^{+\infty} \left|\xi_{rs}(\tau, f)\right|^2 e^{-j2\pi(\tau u + f v)} d\tau\, df\right|$$

$$= \left|A_s(v, -u)\, A_r(-v, u)\right| \tag{10}$$

where A_s and A_r are the auto-ambiguity functions of the transmitted and received signals, respectively. The slope of main ridge of $|F(u, v)|$ could be estimated using LSE technique. This technique could also be applied in the case of multiple targets. The slope of the main ridge in (10) can be deduced as

$$m = \frac{2\pi^2\beta}{(\gamma^2 + \pi^2\beta^2)(1+\alpha^2)} \tag{11}$$

Using the approximate angle θ_a, we will now demonstrate how RAT can be efficiently used to estimate multiple targets.

Computing RT of NAF at an angle θ_a is equivalent to computing the projection of rotated-NAF of the dechirped signal at θ_a. Here, rotated-NAF is computed by dechirping both the transmitted and the received signals. The projection of rotated-NAF on f axis could be computed efficiently using the dechirp technique as follows. The square modulus of NAF between $x(t)$ and $y(t)$ is defined as

$$\left|\xi_{xy}(\tau, f)\right|^2 = \left|\int_{-\infty}^{+\infty} y(t)\, x^*(t-\tau)\exp(-j2\pi f t)\, dt\right|^2 . \tag{12}$$

Taking integration in both sides of (12) with respect to τ

$$\Psi(f) = \int_{-\infty}^{+\infty}\left|\int_{-\infty}^{+\infty} y(t)x^*(t-\tau)e^{-j2\pi f t}dt\right|^2 d\tau = \left|X(f)\right|^2 \otimes \left|Y(f)\right|^2 \tag{13}$$

where $x(t)$ and $y(t)$ are the dechirped transmitted and received signals, respectively; $X(f)$ and $Y(f)$ are the FFT of $x(t)$ and $y(t)$, respectively; and the sign $\otimes$ denotes convolution. Using (13) the projection of rotated-NAF (single slice RAT) could be efficiently computed due to the FFT-based processing. Using θ_a and the peak position f_p in (13), we can calculate ρ_p using the geometrical relation $\rho_p = f_p \sin\theta_a$.

Fig. 2 (right window) shows the RAT of Fig. 1 by using only one slice at an angle θ_a. There, we can clearly see the three peaks corresponding to three targets. Fig. 2 (left window) is generated from the entire RAT and Fig. 2 (right window) is generated from only one slice of RAT but they both show the existence of three targets. From the single RAT slice three peak positions for radius ρ_{pi} could be estimated. Then using the line in (9), a *1-d* search on WAF could be used to estimate the parameters. (The three search lines are shown in Fig. 3.) The necessary steps, and the *type of processing*, for estimating parameters from the single slice of RAT are as follows:

- Estimate a projection angle θ_a (*using 2-d FFT and the LSE technique*).
- Compute the single slice RAT of Fig. 1 at the angle θ_a as in Fig. 2 (right) {*efficient dechirp technique via* (13)}.
- Perform a *1-d* search on the RAT slice to find ρ_{pi}.
- A *1-d* search in Fig. 3 along the line $\rho_{pi} = \tau_i \cos\theta_a + (\alpha_i - 1)k\sin\theta_a$ to estimate the peak positions of each target, τ_i and α_i.

The line search in Fig. 3 can also be efficiently implemented without computing the whole WAF. Instead of computing the entire WAF we can compute *1-d* WAF along the straight lines indicated in Fig. 3. From (9), the equation of the straight line which passes along the main ridge (see Fig. 3), can be defined as

$$\alpha = -\frac{\tau}{k}\cot an\theta + \frac{\rho_p}{k\sin\theta} + 1 . \tag{14}$$

Therefore, using (4) and (14), the WAF could be efficiently evaluated for a *1-d* search in the vicinity of the approximate parameters. Fig. 4 shows the block diagram detailing the computation sequences of the proposed algorithm.

5. RESOLUTIONS AND THE EFFECT OF THE INTEGRATION LENGTH OF RAT IN NOISE

In this paper we have used RAT as a square-law detector since it performs better than envelope detector for stronger or equal strength LFM signal detection [2]. The 3-dB response width of ρ from (7) for a given $(\tau = 0, \alpha = 1)$ can be deduced as

$$\Delta\rho = \sqrt{\frac{3\gamma F_s^2(\gamma^2+\pi^2\beta^2)\ln(10)}{5\{2\pi^2\beta^2(\gamma^2+\pi^2\beta^2)+\gamma^4\}}}\ . \tag{15}$$

The 3-dB width can be considered as a measure of selectivity of the estimation [2]. When γ is zero, $\Re(\rho,\theta)$ becomes a delta function. Fig. 5(a) and (b) show the resolution of RAT for a single target. As expected, the peak position shows the exact location of the target in both ρ and θ domain. Fig. 6(a) shows the result of a bicomponent signal. From Fig. 5(a), (b), and 6(a), we can say that RAT provides very high resolution.

The effect of the integration length of RAT in complex white Gaussian noise is discussed here. Due to the space limitation we are not able to show the statistical derivation of RAT. Therefore, we only present the final result. The performance of the detection process can be expressed as

$$\eta = \frac{|E(\Re\,|\,H_1)-E(\Re\,|\,H_0)|}{\left\{\frac{1}{2}[\mathrm{var}(\Re\,|\,H_1)+\mathrm{var}(\Re\,|\,H_0)]\right\}^{1/2}}\ . \tag{16}$$

Thus, the effect of the integration length T on the detection performance can be deduced as

$$\eta = \frac{A^2\sqrt{\pi\sqrt{\pi/d}/\gamma}\ erf\left\{T\sqrt{d\gamma}\right\}/N_0}{\left\{\int_{-\sqrt{\gamma}T}^{+\sqrt{\gamma}T}\left[erf\left\{\sqrt{d}\,(\sqrt{\gamma}T+u)\right\}+erf\left\{\sqrt{d}\,(\sqrt{\gamma}T-u)\right\}\right]du\right\}^{1/2}} \tag{17}$$

where A is the signal's amplitude, F_s is the sampling rate, $d=\gamma/2F_s^2$, and T is normalized by $\sqrt{1/\gamma}$.

Fig. 6(b) shows the performance of detection of RAT in white Gaussian noise with the variation of integration length T. There it can be seen that the detection performance increases as T increases and it reaches its maximum value at an optimal length $T_{opt}=12$. Further increasing T degrades performance and it approaches to zero as T approaches to infinity.

6. SIMULATION RESULTS

The received signal $x(t)$ is modeled as a linear sum of three wideband GLFM signals with Doppler stretches and time delays α_i and τ_i respectively and corrupted by additive white Gaussian noise $n(t)$ with standard deviation σ_n

$$x(t)=\sum_{i=0}^{2}\exp\left\{-\gamma\alpha_i^2(t-\tau_i)^2+j[2\pi\kappa\alpha_i(t-\tau_i)+\pi\beta\alpha_i^2(t-\tau_i)^2]\right\}+n(t) \tag{18}$$

To demonstrate the superiority of the RAT we consider three point targets where two of them are slightly overlapping to each other and the third one is also close to them (see Fig. 1). The parameters used to obtain Fig. 1 are: $k=200$, $\beta=300$, $\gamma=10\pi$, signal duration $T_s=1\sec$, and $F_s=1kHz$.

Fig. 7 and 8 show the simulation results of estimating Doppler stretch and time delay respectively of the three point targets. The mean square error (MSE) of the proposed estimator of τ and α is also compared with the CRLB. The comparisons are based on 500 independent trials. The CRLB's of τ and α are given by

$$CRLB(\tau)=\frac{10^{-SNR/10}(\pi^2\beta^2\gamma+\gamma^3+2\pi^2k^2\gamma^2)/2}{\alpha^2(\gamma^4+2\pi^2\beta^2\gamma^2+2\pi^2k^2\gamma^3+\pi^4\beta^4)} \tag{19}$$

$$CRLB(\alpha)=\frac{\alpha^2 10^{-SNR/10}(\gamma^4+\pi^2\beta^2\gamma^2)}{(\gamma^4+2\pi^2\beta^2\gamma^2+2\pi^2k^2\gamma^3+\pi^4\beta^4)} \tag{20}$$

The signal-to-noise ratio (SNR) is defined as signal energy to noise power, which is the total SNR. Simulations show that, for (τ_0,α_0) = (-0.06, 1.0), i.e. well separated targets, the estimator closely meet the CRLB in high SNR. On the other hand when targets are not well separated, for (τ_1,α_1) = (-0.22, 0.95) and (τ_2,α_2) = (-0.08, 1.08) the estimation error difference with the CRLB is about 20dB. This is mainly due to the bias incurred by the other target. It can also be seen that when SNR<10dB the target parameters can not be estimated accurately [7]. (Note that the CRLB is shown for $\alpha=1$ because the CRLB's are almost the same for all the three targets.)

7. CONCLUSION

An efficient technique based on single slice RAT for time delay and Doppler stretch estimation has been presented in this paper. The proposed approach combines the modulus square of NAF, the modulus square of WAF, and the Radon transform to estimate multiple GLFM sonar target parameters in noisy environments. Simulation results have been presented to show the effectiveness of the proposed technique.

8. REFERENCES

[1] J. C. Wood, and D. T. Barry, "Radon transformation of time-frequency distributions for analysis of multicomponent signals," *IEEE Trans. Signal Processing*, vol. 42, no. 11, pp. 3166–3177, 1994.

[2] Minsheng Wang, A. K. Chan, and C. K. Chui, "Linear frequency-modulated signal detection using Radon-ambiguity transform," *IEEE Trans. Signal Processing*, vol. 46, no. 3, pp. 571–586, 1998.

[3] B. K. Jennison, "Detection of polyphase pulse compression waveforms using the radon-ambiguity transform," *IEEE Trans. Aerospace and Electronic Systems*, vol. 39, no. 1, pp. 335–343, Jan. 2003.

[4] M. R. Sharif and S. S. Abeysekera, "Efficient wideband signal parameter estimation using combined narrowband and wideband ambiguity functions," *IEEE Pacific Rim Conference on Communications, Computers and Signal Processing*, vol. 1, pp. 426–429, Victoria, BC, Canada, Aug. 2003.

[5] S. S. Abeysekera and M. R. Sharif, "Efficient time delay and Doppler stretch estimation of wideband sonar signals using the Radon-ambiguity transform," *The 8th World Multi-Conference on Systemics, Cybernetics and Informatics*, Florida, USA, July 2004.

[6] L. G. Weiss, "Wavelets and wideband correlation processing," *IEEE Signal Processing Magazine*, pp. 13–32, Jan. 1994.

[7] D. W. Tufts, H. Ge, and S. Umesh, "Fast maximum likelihood estimation of signal parameters using the shape of the compressed likelihood function," *IEEE Journal of Oceanic Engineering*, vol. 18, no. 4, pp. 388–400, 1993.

[8] G. F. Boudreaux-Bartels and P. J. Wiseman, "Wigner distribution analysis of acoustic well logs," in *Proc. IEEE ICASSP*, Dallas, TX, April 1987.

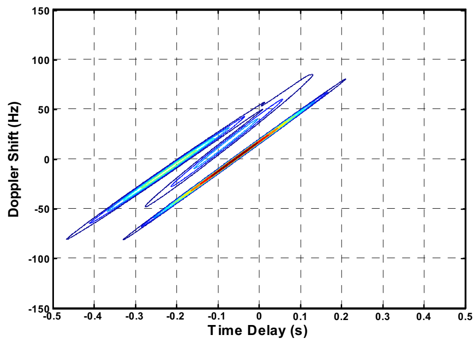

Fig. 1. Contour plots of NAF in the presence of three targets. The target parameters are (τ_0, α_0) = (-0.06, 1), (τ_1, α_1) = (-0.22, 0.95), and (τ_2, α_2) = (-0.08, 1.08).

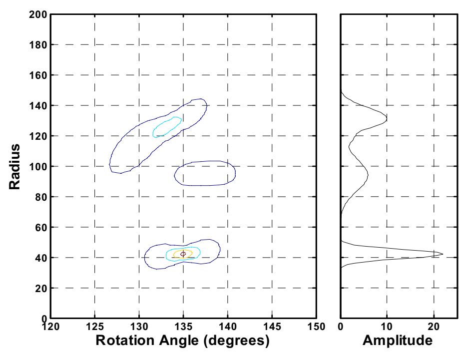

Fig. 2. Entire RAT of Fig. 1 (left window) and single slice RAT of Fig. 1 at the angle $\theta_a = 135°$ (right window).

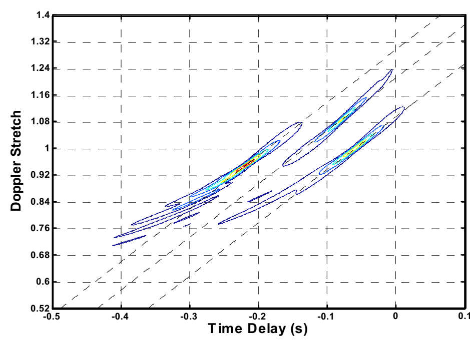

Fig. 3. Contour plots of WAF of the same signal as in Fig. 1 and the three search lines.

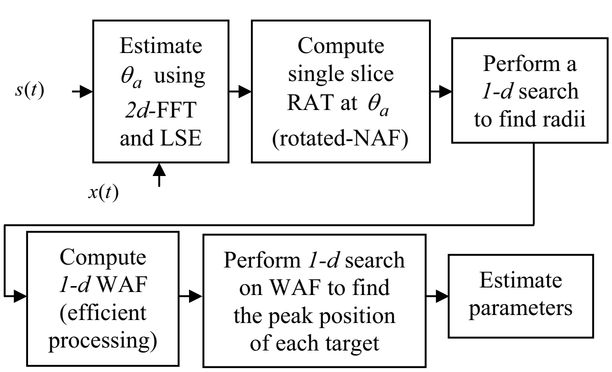

Fig. 4. Block diagram of the proposed method.

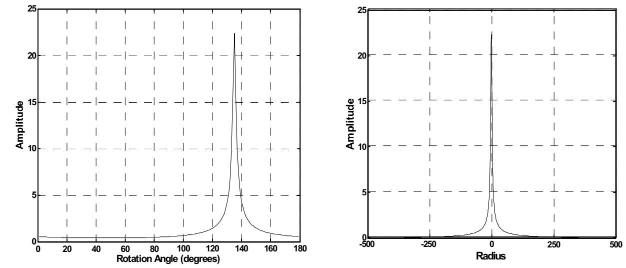

(a) (b)

Fig. 5. Resolution of RAT for a single target. The parameters are (α_0, τ_0) = (1, 0). Expected $(\theta_0, \rho_0) = (135^0, 0)$. (a) Rotation Angle versus Amplitude, (b) Radius versus Amplitude.

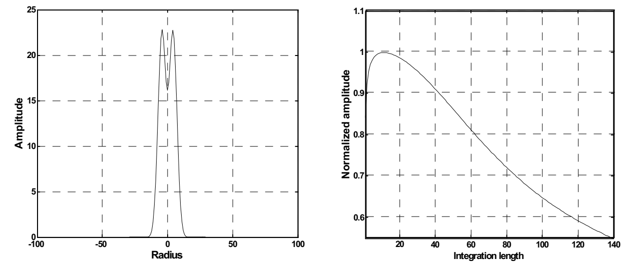

(a) (b)

Fig. 6. (a) Resolution of RAT for a bicomponent signal in ρ (radius) domain. The two targets parameters are (τ_0, α_0) = (0.006, 1) and (τ_1, α_1) = (-0.006, 1). (b) Detection performance of RAT with the variation of the integration length T.

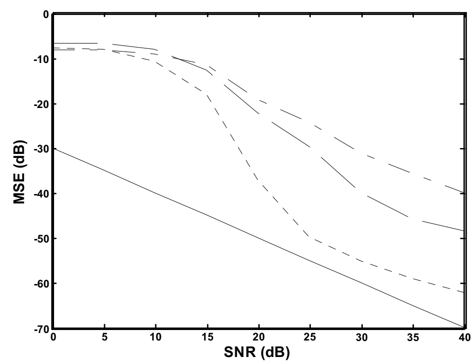

Fig. 7. MSE of estimating α_i against total SNR. Dotted line: (τ_0, α_0) = (-0.06, 1), Dashed line: (τ_1, α_1) = (-0.22, 0.95), Dash-dotted line: (τ_2, α_2) = (-0.08, 1.08), Solid line: CRLB.

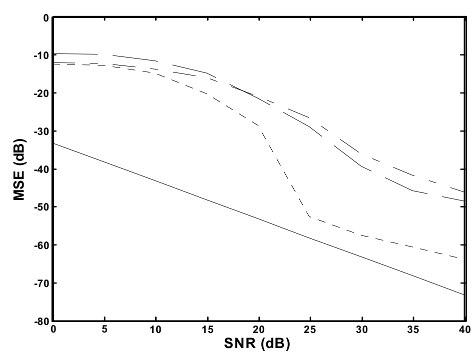

Fig. 8. MSE of estimating τ_i against total SNR. The parameters and the definition of the lines are the same as in Fig. 7.